A Novel Optical Gauge for Measuring Coil Strain during Thermal Cooldown and Energization

M'hamed Lakrimi, Scott Baxter, Adrian M. Thomas, Yunxin Gao, Hugh Blakes, Paul Gibbens, and MengChe Looi

***Abstract*—We report on the first operation of a low cost and easy to use novel Fiber Optic Strain Gauge (FOSG) in cryogenic and high magnetic field environments. Before its deployment on coils, the gauge was first validated on an aluminum cantilever to show that the strain measured is indeed independent of temperature for a given load or deflection. The FOSG is shown not to be affected by background magnetic field.**

Four strain gauges were then mounted on a superconducting coil which was impregnated in epoxy resin. The strains were monitored during every stage of the coil build and we show, for example, that upon post gel resin polymerization shrinkage and with the coil at room temperature, the resin contraction strains in the axial direction is about three times that experienced in the hoop direction. The FOSGs successfully monitored the thermal contraction strains during cryogenic cooldown to 4.2K of the coil and the subsequent electromagnetic strains during energization to several currents. The coil was then deliberately quenched, in excess of 200 times, and again the FOSGs were able to detect the quenches and measure the thermal expansion-induced strains and subsequent re-cooling of the coil after a quench. FEA modeling yielded very good agreement with measured thermal contraction and energization strains.

***Index Terms*—Strain Measurement, Optical Interferometry, Superconducting Magnets, Cryogenics**

I. INTRODUCTION

MAGNETS consist of several inductively coupled coils. A magnet is built to occupy the least volume and to a certain cost for it to be commercially viable. Although a typical customer may only be interested in the specifications of the magnetic field intensity, homogeneity, drift, and temperature of operation, the magnet designer has to adhere to several other requirements for operating current, strain/stress, stray field, typically known as design limits to give the magnet the best probability of making it to field without suffering any training or fatal mechanical damage. Designers continually refine their design limits through observing the performance of magnets and the measurements of certain parameters such as strain which will form the subject of this paper.

Within one magnet, there may be several coil designs. The designer may choose to wind the coil on a former of specific material or not, use wire of a particular geometry and insulation, impregnate the coil to limit any wire motion, etc. Without adding the complication of overbinding and other refinements, it suffices to say that each individual coil is actually a complex composite that may not necessarily be easy to model *a priori*.

Superconducting magnets are designed to operate at low temperatures and thus experience two types of stresses. Firstly, during cooldown, the coils mostly contract, resulting in negative strains. Secondly, during energization, the coils experience intense magnetic forces whereby the coils expand radially thus inducing a positive strain and simultaneously contract axially resulting in a negative strain. In addition, it is also well known that if the local temperature exceeds that of superconducting wire field critical temperature over a critical length then the wire undergoes a transition to normal state and current will be dissipated through the resistive matrix, leading to excessive heating of the coil. This is termed a quench and the magnet suddenly releases its stored energy and a complex quench scenario ensues whereby a particular coil could be magnetically pumped up by its adjacent coils, leading it to experience higher stresses than intended. The designer is therefore concerned whether, after energisation and quench, coils suffer elasto-plastic deformation. It is therefore of paramount importance to accurately measure the strains experienced by coils during operation, ideally using sensors that are not affected by temperature and magnetic field and innovation has played a massive role towards this goal. Conventional resistive strain gauges were found to be very difficult to use because of the temperature and magnetic field corrections [1]. Fiber Bragg Gratings have been extensively used because optical gauges suffered no electromagnetic interaction and several gratings could be written on one fiber [2]-[7]. These sensors were successfully used to characterize coils. However, FBG's are fabricated to suit and analysis of data still required specialized knowledge.

OpSens recently introduced a low cost and off-the shelf

Manuscript received 3 August 2010. This work was supported by the Siemens Magnet Technology student placement scheme.

M. Lakrimi, A. M. Thomas, Y. Gao and H. Blakes are with Siemens Magnet Technology, Wharf Road, Eynsham, Witney, Oxon, OX29 4BP, UK (phone: 44-1865-850394; fax: 44-1865-850178; e-mail: mhamed.lakrimi@siemens.com).

S. Baxter is with The Department of Physics, The University of Bath, Bath, BA2 7AY, UK.

P. Gibbens is with Accurate Controls Ltd, 25 Cowley Road, Nuffield Industrial Estate, Poole, Dorset, BH17 0UJ, UK

M. Looi is with OpSens, 2014 Cyrille-Duquet Street, Québec, G1N 4N6, Canada.

uniaxial optical gauge that is insensitive to transverse strain [8]. The gauge could measure up to 12,000με with a resolution of 0.5με. The only drawback is that one sensor is required per measurement. In this paper, we demonstrate that the sensor is insensitive to temperature and magnetic field. Sensors were mounted on a NbTi-superconducting coil and measured the strains during thermal cooldown and energization. Finite Element Analysis (FEA) was used to model the coil and excellent agreement was found with measurement. Furthermore, the strain gauge detected a quench and from the measurement the temperature attained by the coil is deduced.

II. The Optical Strain Gauge

The strain gauge exploits white light polarization and is based on the principle of a Fabry-Pérot interferometer [9]. As shown in Fig 1, the sensor is placed at the end of the fiber which is sheathed for robustness and the other end is fitted with an optical coupler for connection to a signal analyzer. The cavity is formed by a gap with a nominal spacing between the two end of fibers coated with a dielectric mirror. The two fibers are then enclosed in a 9mm Quartz microcapillary tube. The resulting optical path difference between two beams of

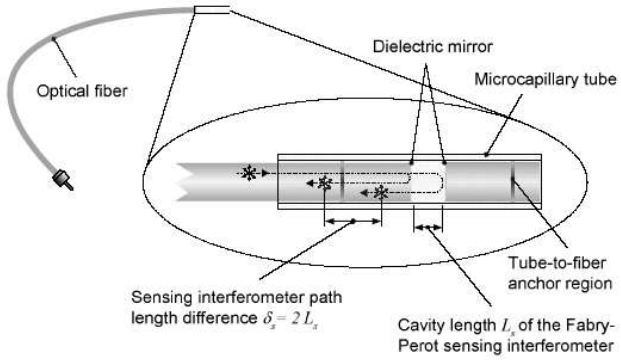

Fig. 1. Schematic diagram of the FOSG showing the location of the cavity and illustrating the path difference between two beams.

light is double that of the cavity length. The strain is simply given by the cavity length divided by the length of the tube. The strain logger directly displays the strain, just like a digital voltmeter displays a voltage without any further processing.

III. Temperature Dependence

To establish the temperature dependence of the strain gauge, a 1050A grade (99.5% purity) aluminum cantilever set-up was used as shown in Fig 2. The FOSG was glued onto the Al plate using Stycast 2850FT and Catalyst 24LV. A copper tube helped support and ensured smooth bending of the fiber. In response to a given weight placed on a load bearing plate, a rod tip induces a deflection on the Al cantilever. A calibrated Linear Voltage Displacement Transducer (LVDT) mounted on the load bearing plate was used to measure the deflection. It is known that the elastic one dimensional straight beam gives the temperature independent strain at axial position *x* as [12]

$$\varepsilon = \frac{18I}{wt^2}\frac{(l-x)}{l^3}y \qquad (1)$$

where *I*, *l, w, t,* and *y* are the moment of inertia of the beam, length, width, thickness of the cantilever, and the vertical

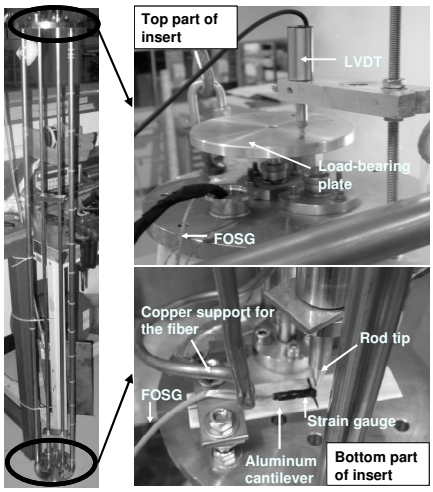

Fig. 2. Cantilever set up showing the top plate for loading weights and the rod tip which inflicts a defection onto the aluminum plate.

deflection of the cantilever tip, respectively. Fig 3 confirms the temperature independence of the strain gauge. In addition the thermal contraction was measured as 0.42% [10] and this is in very good agreement with that of pure Al [11].

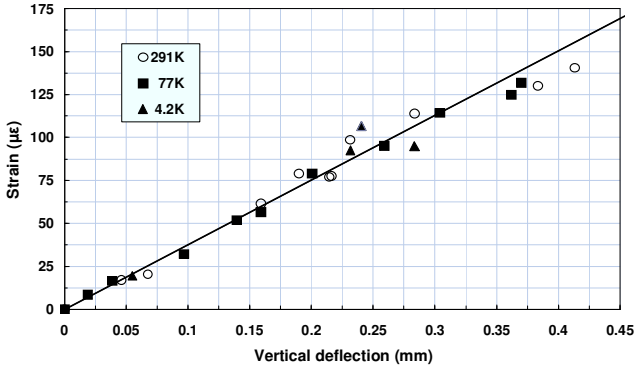

Fig. 3. The strain-deflection does not depend on temperature as predicted by Eq 1. The straight is a fit to the data using x=30.65mm.

It was further established that a small rotation of ±10° of the load bearing plate resulted in an error in the displacement of 50μm because the plate was not welded horizontally. In order to make the rod move freely, the holes were slightly enlarged and this can easily make the rod tip move freely from intended position. An FEA model estimated that a 6mm off the centre location of the rod tip would yield the strain to decrease by 13μm. It can be seen that once these errors are taken into account the data would be much closer to the theoretical line.

IV. Measuring the Strain on a Coil

After further establishing that the FOSG response is independent of magnetic field when inserted in the bore of an MRI magnet, four sensors were mounted on a one third scale superconducting coil. The 63.2mm wide coil which had an inner and outer radius of 168mm and 182.4mm, respectively, consisted of 10 layers of 28 turns of braid insulated Cu/NbTi wire wound onto an Al former. Two sensors were located on top of the second last layer of the winding and were fixed in place on the axial and radial axes. The sensing part being fragile, it is the sheathed part of the fiber that is bent to align the measuring cavity along the intended directions. After

protecting the sensors from being crushed by the tension-induced load of the last wire layer from crushing them, the final layer of wire was then wound and another pair of sensors was similarly laid on top of this last layer. Once vacuum impregnated, the coil was heated to 90°C for several hours to cure the epoxy resin. The excess resin was then hot-stripped from the coil. The strains measured by the four gauges were monitored after completion of each process stage of the coil construction. Fig 4 is a plot of the observed strains and shows that these were grouped in pairs, with the axial gauges measuring much greater values than those in the radial direction and this is attributed to resin polymerization volume shrinkage [13]-[15]. Close examination of the data in Fig 4 shows that the small difference between the two Hoop gauges started after post winding which shows that the top two gauges have been slightly disturbed, probably during handling unlike the bottom gauges which are held in place by the last layer of winding. The reading of the top hoop gauge runs parallel to that under the last layer after post winding otherwise both gauges would have shown perfect agreement.

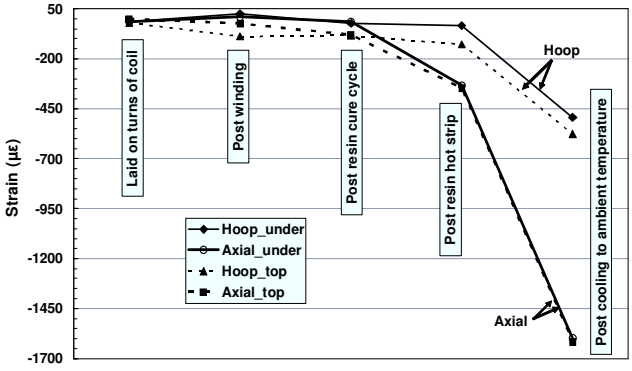

Fig. 4. Logged strains from winding to post cooling to ambient temperature where resin would have cured and undergone maximum volume shrinkage.

With hindsight, it is understandable that the two axial gauges measured similar strains with a larger contraction than those along the hoop direction. This is due to the relative resistance to resin contraction the wire provided on the two axes. In the hoop direction, the resin contraction was restricted by the unbroken lengths of the turns of wire which contracted far less than the resin as it cooled to ambient temperature. In the axial direction the resin contraction was only resisted by the widths of the wire; gaps between each turn of the wire along a layer were resin filled. As a result, resin between layers gaps contracted axially unimpeded and the two gauges give exactly the same reading.

During cooldown to 4.2K this pairing of the measurements continued as shown in Fig 5. However, the difference between values from gauges of the same direction started to open up. Cu/NbTi is well known to contract less than epoxy resin and thus the reduced values measured by the sensors under the last layer compared to the values measured by the gauges above the last layer of winding. The sensors on the last layer are surrounded by a greater volume of resin than the sensors located between layers. Evans showed that the mechanical properties of resin depend on its thickness and more strain will be measured in regions where resin is the thickest [13].

The coil was subsequently energized to different operating

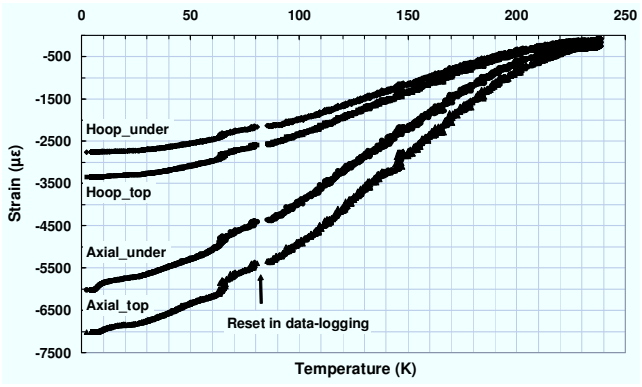

Fig. 5. Pairing of the axial and radial strains continued during thermal cooldown to 4.2K of the coil.

currents using a ramp rate of 500A/min and then deliberately quenched using a variety of heaters. Upon energization, the coil expanded in the hoop direction forcing the turns to be under tension, resulting in a positive strain. At the same time

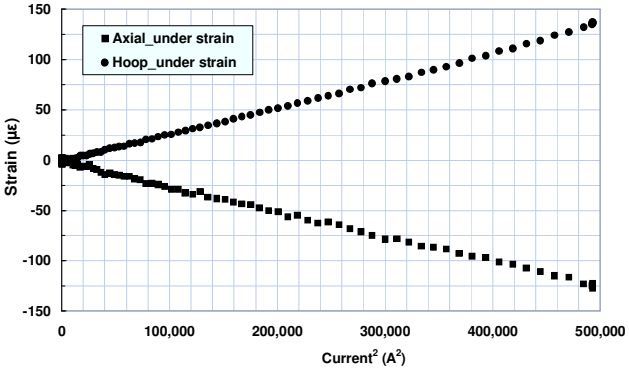

Fig. 6. The Hoop and axial strains follow the expected I^2-dependence.

the coil contracts axially, resulting in a negative strain. The strain is also well known to depend on the square of the magnetic field intensity or the current and Fig 6 shows the Hoop and axial strains follow such behavior.

A mechanical-magnetic coupled FEA model was used to estimate the expected strains in the hoop and axial axes in the coil. The material parameters were calculated using the Halpin-Tsai equations [17] and the so called *rule of mixtures* [18]. The material parameters were taken from the literature [13], [16]. Table I gives the results of the calculation and the agreement with theory is very good [10].

TABLE I MEASURED AND CALCULATED HOOP AND AXIAL STRAINS DURING COOLDOWN AND COIL ENERGIZATION

Strain gauge	Strains due to cooldown from 300K to 4.2K [με]		Strains due to magnetic load at 400A [με]		Strains due to magnetic load at 700A [με]	
	Meas	Calcul	Meas	Calcul	Meas	Calcul
Axial_und	-7012	-6315	-47	-39	-124	-118
Hoop_und	-2758	-3593	+38	+47	+137	+147
Axial_top	-6018	-6159	-33	-31	not meas.	-94
Hoop_top	-3354	-3606	+45	+49	not meas.	+151

The strains were referenced to those at room temperature.

Finally, Fig 7 shows the coil energization to 500A (top trace) and 700A (bottom trace) as a function time using the

same scales for ease of comparison. For the 500A traces, the strains are as given by the data logger whereas for the 700A traces, the strains were offset to zero at the start of the current ramp. The axial and hoop strains follow their usual behavior described in Fig 6. After reaching the set current, the coil is deliberately quenched using a heater. As a result of the quench the current is dissipated in the wire matrix causing the temperature of the coil to rise and at the same time the magnetic pressure collapses to zero. As the magnetic pressure collapses to zero the radial strain collapses towards zero and the coil should normally recover its original length before energization. However this recovery is hampered by the heating of the coil through the current dissipation that takes the coil to a higher temperature first and of course, the coil slowly cooldown again back to 4.2K because it is immersed in liquid helium. It is well know that a quench from 500A will heat the coil less than a quench at 700A due to Joule heating;

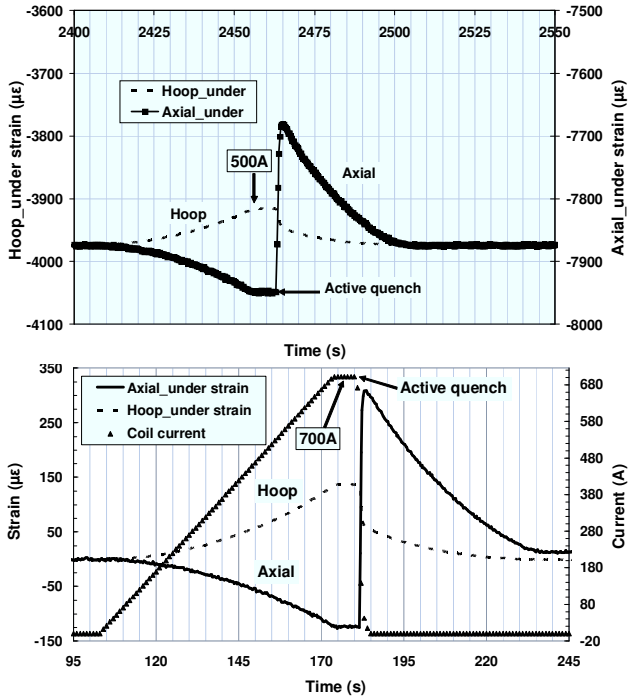

Fig. 7. The Hoop and axial strains during energization to 500A (top trace) and 700A (bottom trace) followed by a deliberate quench of the coil.

it is very apparent from Fig 6 that indeed the axial reading strain reached by the coil immediately after the initiation of the quench is less in the quench at 500A compared to that at 700A. Furthermore, the data shows that during the quench at 700A, the coil takes 55s to cool down back completely to 4.2K compared to only 40s during the quench at 500A, again indicating that the heating was greater during the quench at 700A. Given the strains reached during quench, it could be argued that the coil reached a temperature reached at 700A is roughly 40K.

V. Conclusion

A new optical fiber based strain gauge has been shown to be operating in a cryogenic and magnet field environment. The sensors were successfully deployed on a superconducting coil impregnated with epoxy resin. The strain gauges measured resin shrinkage and strains during coil energization. Furthermore the sensors successfully captured quench events and the resulting heating and subsequent cooldown of the coil.

Acknowledgment

S. Baxter would like to thank Siemens Magnet Technology for the award of a six month work placement. We would like to thank the following for their valuable assistance: N. Belton for the loan of the insert, B. Jones and A. Shepheard for coil preparation, Stuart Smith for coil impregnation, and the coil winding cell.

References

[1] J. Kondo, "Resistance minimum in dilute magnetic alloys," *Prog Theor Phys* vol. 32, pp. 7-49, 1964.

[2] S. W. James, R. P. Tatam, A. Twin, M. Morgan, P. Noonan, "Strain response of fiber Bragg grating sensors at cryogenic temperatures," *Meas. Sci. Technol.* Vol. 13, pp. 1535-39, 2002 and references therein.

[3] R. Rajinikumar, K.G. Narayankhedkar, G. Krieg, M. Süßer, A. Nyilas, K.P. Weiss, "Fiber Bragg gratings for sensing temperature and stress in superconducting coils," *IEEE Trans Appl Supercond* vol. 16, pp. 1737-40, 2006.

[4] I. Latka, W. Ecke, B. Höfer, T. Habisreuther, R. Willsch, "Fiber-optic Bragg gratings as magnetic field-insensitive strain sensors for the surveillance of cryogenic devices," *Cryogenics* vol. 49, pp. 490-96, 2009.

[5] M. Willsch, Hertsch, T. Bosselmann, M. Oomen, W. Ecke, I. Latka, H. Höfer, "Fiber optical temperature and strain measurements for monitoring and quench detection of superconducting coils," *Proc SPIE* vol. **7004**:70045, pp. G-1-4, 2008.

[6] R. Rajinikumar, M. Süßer, K. G. Narayankhedkar, G. Krieg, M. D. Atrey, "Design parameter evaluation of a metal recoated Fiber Bragg Grating sensors for measurement of cryogenic temperature or stress in superconducting devices," *Cryogenics* vol. **49, pp.** 202-09, 2009.

[7] E. Chehura, S. James, A. Johnstone, M. Lakrimi, F. Domptail, A. Twin, R. Tatam, "Multi-component strain development in superconducting magnet coils monitored using fiber Bragg grating sensors fabricated in highly linearly birefringent fiber", Submitted to the Journal of Smart Materials and Structures, 2009, and references therein.

[8] OpSens Inc. (Canada) online datasheet, *Fiber optic strain gauge datasheet*. Available from: http://www.opsens.com/pdf/products/OSP-A%20Rev%201.5.pdf.

[9] OpSens Inc. (Canada) online report, *White light Interferometry*. Available from: http://www.opsens.com/pdf/WLPIREV2.3.pdf.

[10] S. Baxter, M. Lakrimi, A. M. Thomas, Y. Gao, H. Blakes, P. Gibbens, M. Looig, "Validation of a novel fiber optic strain gauge in a cryogenic and high magnetic field environment," submitted to Cryogenics, 2010.

[11] R. P. Reed, A. F. Clark, *Materials at low temperatures*, American Society for Metals, Metals Park, OH: 1983, pp. 8, pp. 95.

[12] W. Young, R. Budynas, *Roark's formulas for Stress and Strain*, 7th Ed. Singapore: McGraw-Hill, 2002, pp. 126-128, pp. 189, pp. 802.

[13] D. Evans, "Material Technology for Magnet Insulation and Bonding," *IEEE Trans Appl Supercond* vol. 10, pp. 1300-05, 2000.

[14] C. Li, K. Potter, M. R. Wisnom, G. Stringer, "In situ measurement of chemical shrinkage of MY750 epoxy resin by a novel gravimetric method," *Cryogenics* vol. 64, pp. 55-64, 2004.

[15] S. V. Hoa, P. Ouelette, T. D. Ngo, "Determination of shrinkage and modulus development of thermosetting resins," *J. Composite Mat* vol. 43, pp. 783-803, 2009.

[16] M. Wilson, *Superconducting Magnets*. Oxford: Clarendon Press, 1983, pp. 41-47.

[17] J. C. Halpin, J. L. Kardos, "The Halpin-Tsai equations: a review," *Polymer Engineering and Science* vol. 16, pp. 344-52, 1976.

[18] R. M. Jones, "Mechanics of Composite Materials. McGraw-Hill, New York: 1975.

[19] E. S. Bobrov, J. E. C. Williams, Y. Iwasa, "Experimental and theoretical investigation of mechanical disturbances in epoxy-impregnated superconducting coils. 2. Shear-stress-induced epoxy fracture as the principal source of premature quenches and training - theoretical analysis," *Cryogenics* vol. 25, pp. 307-16, 1985.